JOURNAL OF GEOPHYSICAL RESEARCH, VOL. 106, NO. C5, PAGES 9455–9472, MAY 15, 2001

Temporal and vertical variability in optical properties of New England shelf waters during late summer and spring

Heidi M. Sosik and Rebecca E. Green

Biology Department, Woods Hole Oceanographic Institution, Woods Hole, Massachusetts

W. Scott Pegau

College of Oceanic and Atmospheric Sciences, Oregon State University, Corvallis, Oregon

Collin S. Roesler

Bigelow Laboratory for Ocean Sciences, West Boothbay Harbor, Maine

Abstract. Relationships between optical and physical properties were examined on the basis of intensive sampling at a site on the New England continental shelf during late summer 1996 and spring 1997. During both seasons, particles were found to be the primary source of temporal and vertical variability in optical properties since light absorption by dissolved material, though significant in magnitude, was relatively constant. Within the particle pool, changes in phytoplankton were responsible for much of the observed optical variability. Physical processes associated with characteristic seasonal patterns in stratification and mixing contributed to optical variability mostly through effects on phytoplankton. An exception to this generalization occurred during summer as the passage of a hurricane led to a breakdown in stratification and substantial resuspension of nonphytoplankton particulate material. Prior to the hurricane, conditions in summer were highly stratified with subsurface maxima in absorption and scattering coefficients. In spring, stratification was much weaker but increased over the sampling period, and a modest phytoplankton bloom caused surface layer maxima in absorption and scattering coefficients. These seasonal differences in the vertical distribution of inherent optical properties were evident in surface reflectance spectra, which were elevated and shifted toward blue wavelengths in the summer. Some seasonal differences in optical properties, including reflectance spectra, suggest that a significant shift toward a smaller particle size distribution occurred in summer. Shorter timescale optical variability was consistent with a variety of influences including episodic events such as the hurricane, physical processes associated with shelfbreak frontal dynamics, biological processes such as phytoplankton growth, and horizontal patchiness combined with water mass advection.

1. Introduction

The absorption and scattering properties of the constituents of seawater, which determine optical variability in the ocean, differ in magnitude and scales of variability between oceanic and coastal waters. A more diverse assemblage of optically important material is often present on and near continental shelves, and a wide variety of physical forcing processes directly affect the distribution of this material. In addition to the locally derived phytoplankton (and associated products) that play a critical role in open ocean optics, coastal waters are subject to inputs of terrigenous material and resuspension of sedimented material. These processes can introduce optically important particulate and dissolved material into the water column at a variety of space scales and timescales depending on the local physical regime.

Paper number 2000JC900147.
0148-0227/01/2000JC900147$09.00

Characterization of the optical properties of natural particulate and dissolved material, as well as of the sources and scales of variability in these properties, is important for a variety of applications. These range from basic studies of radiative transfer theory and its application in the upper ocean to issues of biological and chemical significance, including modeling of apparent optical properties such as attenuation of downwelling irradiance and remote sensing reflectance. Penetration of light into the upper ocean is relevant for understanding photosynthesis and other photochemical processes, and there is increasing interest in remotely estimating the abundance of seawater constituents such as phytoplankton pigments and colored dissolved organic matter (CDOM) on the basis of reflectance data. Both diffuse attenuation and reflectance from the ocean surface vary spectrally and are highly dependent on water constituents [e.g., *Morel and Prieur*, 1977; *Smith and Baker*, 1978; *Morel*, 1988]. While the inherent optical properties of water itself are strongly wavelength dependent, absorption and scattering by particulate and dissolved material lead to spatial and temporal variability.

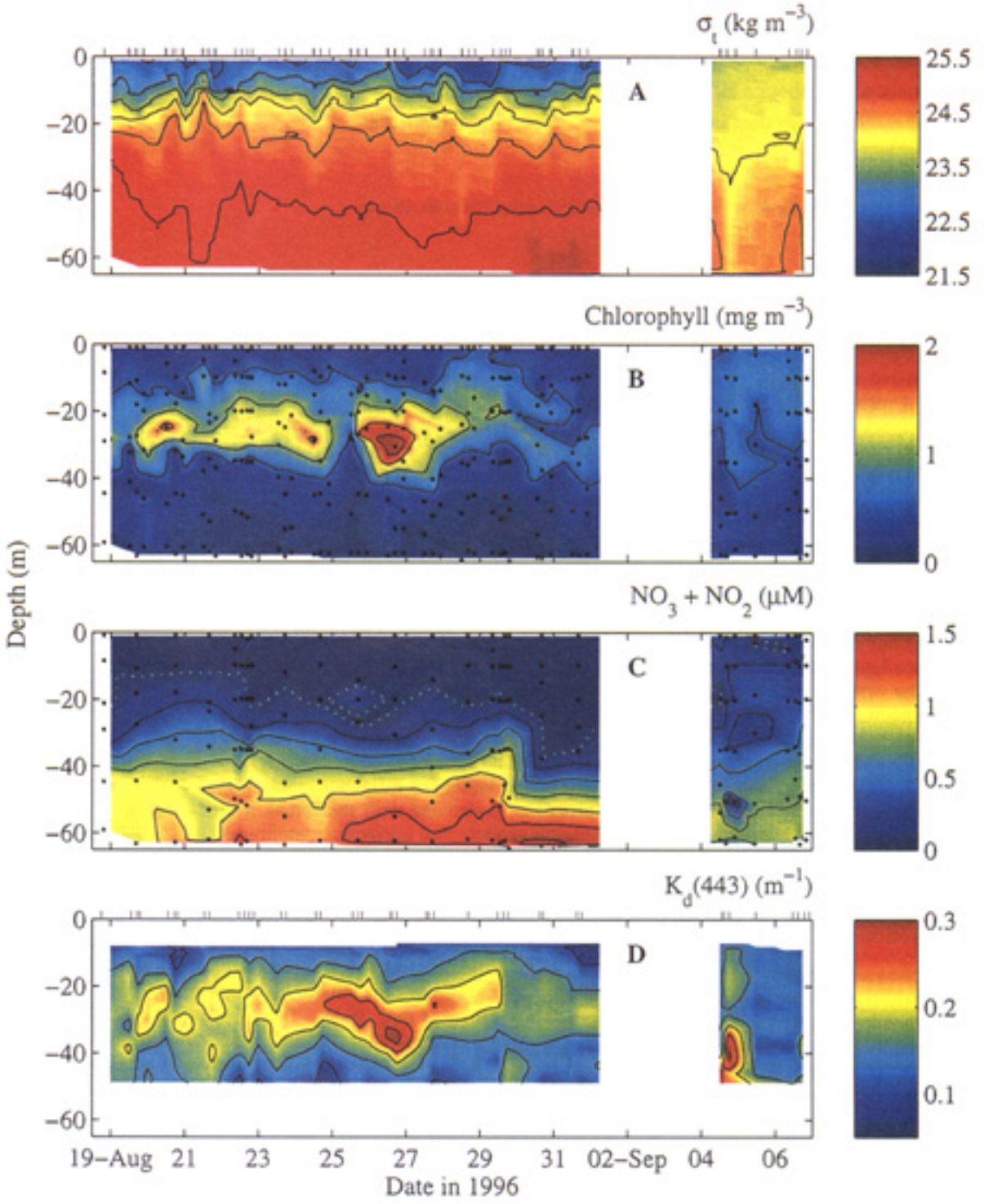

Plate 1. Time series of interpolated water properties at the study site (40°30′N, 70°30′W) during late summer in 1996: (a) Density determined from measurements with the ship's SeaBird CTD during rosette casts to collect discrete water samples, (b) Chl *a* concentration, (c) nitrate plus nitrite concentration, and (d) diffuse attenuation for downwelling irradiance K_d at 443 nm. Contours (solid black lines) are drawn at intervals of 0.05, 0.5, 0.25, and 0.05 in Plates 1a, 1b, 1c, and 1d, respectively, and the 0.05 μM nitrate isoline is also noted in Plate 1c (dotted white line). Discrete sample positions are indicated (black dots) in Plate 1b and 1c and times of continuous profiles are marked (black ticks) above Plates 1a and 1d.

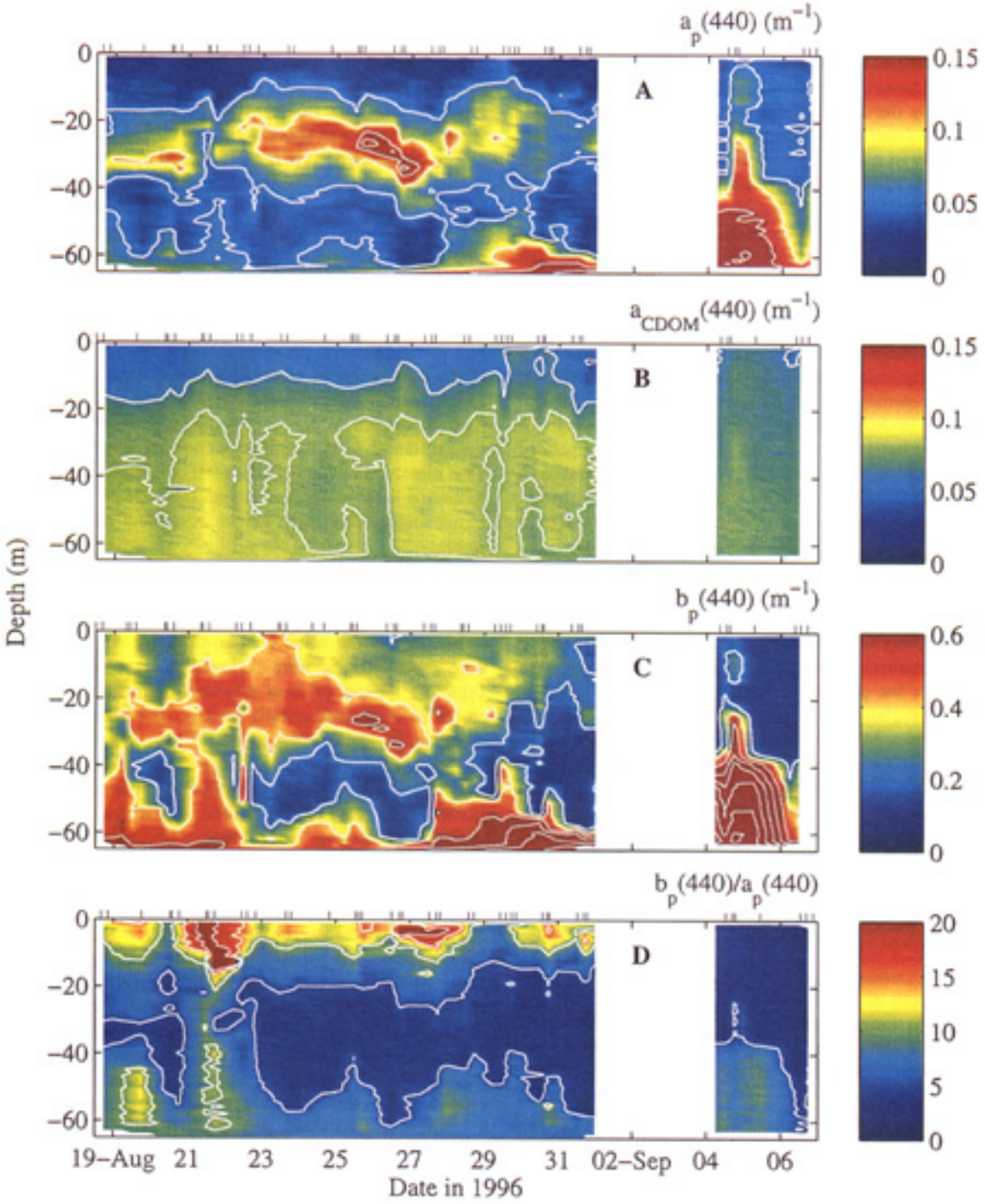

Plate 2. Time series of interpolated inherent optical properties at 440 nm during the same period as in Plate 1: (a) Absorption coefficients for particulate material (a_p), (b) absorption coefficients for dissolved material ($a_{C\text{-}DOM}$), (c) scattering coefficients for particles (b_p), and (d) the ratio of b_p to a_p. Measurements are from in situ profiles with ac-9 instruments on the SlowDROP package. Contours (white lines) are drawn at intervals of 0.05, 0.02, 0.2, and 5 in Plates 1a, 1b, 1c, and 1d, respectively. Timing of vertical profiles is indicated (black ticks) above each panel. Note that b_p values dramatically exceeded 0.6 m^{-1} in the bottom 25 m on September 4-6 (maximum values ~1.5 m^{-1}).

Spatial and temporal variability in the optical properties of coastal regions presents a great challenge toward the parameterization of optical models. Regions such as the New England shelf are among the most productive areas of the world's oceans because of complex interactions between physical and biological processes [*O'Reilly et al.*, 1987]. These complex interactions, however, make optical algorithms for coastal regions among the most difficult to parameterize. For example, Coastal Zone Color Scanner (CZCS) algorithms performed poorly in regions of high chlorophyll *a* concentration [*Gordon et al.*, 1988], high suspended sediment concentration [*Doerffer and Fischer*, 1994], high CDOM concentration [*Carder et al.*, 1989; *Hochman et al.*, 1994], and coccolithophorid blooms [*Holligan et al.*, 1983; *Balch et al.*, 1989], all conditions most often found in coastal regions, including the New England shelf.

The Coastal Mixing and Optics experiment (CMO) was conceived to address some of these issues. The objective of this multidisciplinary program is to quantify and understand the role of vertical mixing processes (in a laterally varying environment) in determining the midshelf vertical structure of hydrographic, optical, and particle properties. As part of CMO, an 11 month observational program was conducted in continental shelf waters south of Cape Cod, Massachusetts. Here we describe results from a component of this program that focused on detailed optical variability at the experimental site during two intensive sampling periods. Our aims are to describe important temporal and vertical variability in optical properties, to identify which seawater constituents contribute most significantly to water column optical variability, and to make an assessment of potential contributing processes. We report that for the period and region examined, particles, in particular phytoplankton, are the major source of variability in optical properties and that physical forcing of optical variability is most evident through responses of the phytoplankton. Extreme events such as the passage of a hurricane represent an exception when direct effects of physical forcing are evident and important temporal and vertical changes in nonphytoplankton material occur.

2. Material and Methods

2. 1. Experiment Site

CMO was carried out at a site on the southern New England shelf, south of Martha's Vineyard (40°30′N, 70°30′W). The site lies in a region known as the "Mud Patch" and has a water depth of ~70 m. A suite of moored array, towed vehicle, and shipboard sampling was made near the site from July 1996 through June 1997 [*Dickey and Williams*, this issue]. The data presented here were collected during two 3 week cruises in the late summer of 1996 aboard the R/V *Seward Johnson* (cruise SJ9610, August 17 to September 7) and spring of 1997 aboard the R/V *Knorr* (cruise KN150, April 24 to May 13). Vertical profiles of optical properties and water-sampling casts were carried out approximately three times per day during daylight hours at the main CMO site, within a few kilometers of 40°30′N, 70°30′W. All dates and times are reported in UTC.

2.2. Sampling

2.2.1. Optical measurements. Sampling for optical properties included in situ profiling to measure both inherent and apparent optical properties, as well as collection of discrete water samples for more detailed laboratory measurements. Apparent optical properties were measured with a tethered free-fall spectral radiometer (SPMR system, Satlantic, Inc.) equipped with seven spectral wavebands (412, 443, 490, 510, 555, 665, and 683 nm; spectral bandwidth, 10 nm). The SPMR system consisted of a profiler that measures downwelling irradiance E_d, upwelling radiance L_u, conductivity, temperature, pressure, and instrument tilt, as well as a reference sensor (SMSR) that floats just below the water surface (30 cm depth) and measures spectral E_d.

The radiometers were hand deployed from the "sunny side" of the ship, and measurements were not collected until enough cable was released so that instruments (the profiler and surface reference) were several tens of meters from the ship to minimize ship shadowing effects on measurements of the underwater light field. The profiler was weighted to fall with a mean vertical velocity of ~1 m s^{-1}, and observations were logged at 6 Hz. Since the profiler is designed to maintain vertical orientation only during free fall, data were collected on downward casts only. Four vertical profiles were usually acquired during each deployment from which a best cast was chosen on the basis of the tilt and vertical velocity of the profiler and the variability of surface downwelling irradiance measured by the surface reference. Both the profiler and reference sensors were calibrated (at Satlantic facilities) precruise and postcruise to assess instrument performance and stability.

Data from the spectral radiometers were processed using software provided by Satlantic, Inc. (ProSoft version 3.5d). All casts were edited to remove contaminated data at the top and bottom of the water column (high tilt and low velocity), were calibrated, and were averaged to 1 m bins over depth z. Typically, the top 5-6 m of data were eliminated from profiles on the basis of these criteria (mean over both cruises was 5.8 m with a standard deviation of 1.7 m). Irradiance and radiance data from the 1996 summer cruise were corrected for zero offset values using laboratory-determined dark measurements. Because of uncertainties in dark values due to factors such as varying water temperature, on the 1997 spring cruise a dark cast was acquired during each deployment by placing black caps over the profiler optical heads; these depth-dependent dark values were then used in deriving calibrated irradiance and radiance profiles. Depth-dependent diffuse attenuation coefficients for downwelling irradiance K_d were computed for each wavelength as $d\{\ln[E_d(z)]\}/dz$ [*Smith and Baker*, 1984; 1986] over eight 1 m depth bins; diffuse attenuation coefficients for upwelling radiance K_u were computed in an analogous manner with L_u substituted for E_d. Remote sensing reflectance R_{rs} was estimated as the ratio of water-leaving radiance to E_d just above the sea surface ($z = 0^+$); values at $z = 0^+$ were estimated by extrapolating from the top of the measured vertical L_u and E_d profiles to $z = 0^-$ using the shallowest K_d and K_u estimates available for each cast, and then assuming Fresnel reflectance for the sea surface of 0.021 for L_u and 0.043 for E_d [*Gordon et al.*, 1988; *Mueller and Austin*, 1995].

Inherent optical properties were measured in situ with dual-path absorption and attenuation meters (ac-9, WetLabs, Inc.). The ac-9 meters are designed to measure absorption a and beam attenuation c coefficients in nine spectral bands, which were selected to complement those of the radiometers: 412, 440, 488, 510, 532, 555, 650, 676, and 715 nm. During both CMO cruises, at least two ac-9 meters were mounted on the Slow Descent Rate Optical Platform (SlowDROP) maintained by the Ocean Optics Group at Oregon State University,

with the exception of the last half of the spring cruise when these sensors were transferred to Texas A&M University's Particle and Optics Profiling System (POPS) designed for video camera work. During most deployments, multiple profiles were acquired, and a single representative cast was selected. The ac-9 sensors were calibrated daily shipboard using water generated with a NANOpure system (Barnstead). Unfiltered and filtered (0.2 μm SuporCap100 cartridge filter, Gelman Sciences) seawater was pumped through two separate ac-9 meters to measure a and c due to all material present in the seawater and to dissolved material only. The contribution of particles to total absorption was assessed as the difference between the unfiltered and filtered values. Temperature and salinity corrections were applied to both absorption and attenuation values [*Pegau et al.*, 1997], and absorption measurements were corrected for scattering errors [*Zaneveld et al.*, 1994]. In addition, the absorption spectra for dissolved material were offset to zero at 676 nm.

2.2.2. Ancillary measurements. Approximately three times per day discrete water samples were collected from six depths throughout the water column using a conductivity-temperature-depth profiler/rosette system equipped with sampling bottles (with silicone o rings and external springs on the summer cruise and Teflon-coated springs on the spring cruise). Material collected on glass fiber filters (GF/F, Whatman) was extracted for 24 hours in cold 90% acetone, and chlorophyll a (Chl a) and phaeopigment (phaeo) concentrations were measured fluorometrically using a Turner Designs Model 10 fluorometer calibrated spectophotometrically with pure Chl a (Sigma Chemical Co.). Approximately 300 observations were made at the central site during the summer cruise, and 360 were made during the spring cruise. Periodically, water samples were frozen for later analysis of nutrient concentrations (~190 samples in summer and 50 in spring). Analyses were conducted manually according to *Strickland and Parsons* [1972] for summer samples (NO_3 plus NO_2) and with an autoanalyzer for spring samples (NO_3, NO_2, PO_4, SiO_4, and NH_4).

Absorption coefficients for particulate material (a_p) collected on GF/F filters were determined spectrophotometrically on shipboard (using a Cary 3E dual beam UV/visible spectrophotometer), with sample and reference preparation as described by *Roesler* [1998]. Subsequent to the initial optical density measurements, filters were extracted in methanol and reanalyzed to determine the residual particulate absorption (a_d) [*Kishino et al.*, 1985]; the absorption coefficient due to methanol extractable phytoplankton pigments (a_{ph}) was estimated by difference between the initial and postextraction measurements. All measurements were relative to a blank filter saturated with filtered seawater, and the average optical density between 780 and 800 nm was subtracted from each spectrum as a wavelength-independent correction for small scattering differences between the blank and sample filters. The path length amplification factor of *Roesler* [1998] was used to correct optical density measurements for particle concentration and filter effects. These absorption measurements were made on ~225 and 290 samples from the central site in summer and spring, respectively.

3. Results

3.1. Time Series of Vertical Structure

3.1.1. Summer 1996. As expected for late summer conditions, the water column was well stratified during the first 2 weeks of the sampling period in August 1996 (Plate 1a). Surface temperature and salinity values were ~19-20°C and 31.5-32 psu, and there was a >10 °C decrease in temperature and ~1 psu increase in salinity with depth over the water column [*Gardner et al.*, this issue]. During this period, Chl a concentrations were typically <1 mg m^{-3} in surface waters (mean of 0.44 mg m^{-3} in top 10 m) with a pronounced subsurface maximum between 20 and 30 m where concentrations were as high as 2 mg m^{-3} (Plate 1b). Nitrate plus nitrite concentrations were depleted in surface waters (below detection limit of 0.03 μM) but increased rapidly below 25 m (Plate 1c). Apparent optical properties of the water column also exhibited stratified structure, with middepth maxima evident in diffuse attenuation coefficients (Plate 1d) and radiance reflectance (not shown) at blue to green wavelengths.

These conditions were dramatically disrupted by the passage of Hurricane Edouard through the study site. The hurricane traveled northward in the western North Atlantic during late August, forcing shipboard operations to be halted late in the day on August 31, and on September 2 the center of the storm (wind speeds ~75 mph) passed within ~100 km of the study site [*Thompson and Porter*, 1997]. For this period, virtuously continuous timeseries of physical and bio-optical properties are described by *Dickey et al.* [1998] and *Chang and Dickey* [this issue]. We returned to the site and resumed sampling on September 4. On August 30-31, only small perturbations in the physical properties of the water column were evident, while the Chl a maximum was barely present and the nitracline had deepened by at least 10 m (Plate 1). In contrast, stratification was severely disrupted by storm action during the period when sampling was curtailed, and by September 4, temperature and salinity varied by <2°C and 0.2 psu over the top 40 m. Consistent with a relatively well mixed water column, nitrate plus nitrite concentrations were no longer below detection in surface waters (Plate 1c), and the subsurface Chl a peak had disappeared, with concentrations <1 mg m^{-3} at all depths (Plate 1b). Following the hurricane, surface values of diffuse attenuation coefficients were moderate, and for ~1 day after sampling resumed a pronounced peak in diffuse attenuation was present below 30 m (Plate 1d). While the effects of the hurricane were dramatic, the summer sampling period was dominated by stratified conditions, which are reflected in the mean properties (Table 1).

Inherent optical properties also varied both vertically and temporally during the late summer sampling period. Mid-water column maxima in both absorption and scattering coefficients due to particulate material (a_p and b_p, respectively) were observed during the period prior to the hurricane (Plates 2a and c). Mean a_p at 440 nm was 0.03 m^{-1} in the surface layer, with values as high as 0.25 m^{-1} in the subsurface peak, while $b_p(440)$ values were typically between 0.2 and 0.4 m^{-1} in surface waters and up to 0.8 m^{-1} at mid-water column. High b_p values (>0.6 m^{-1} at 440 nm) were also frequently found near the bottom, where a_p signals were low to moderate (0.02-0.15 m^{-1} at 440 nm). The ratio of $b_p(440)$ to $a_p(440)$ was highest in the surface layer (mean ± standard deviation = 11.6 ± 21.7 for <20 m) and lowest at mid-water column (mean ± s.d. = 4.4 ± 1.9 for 20-40 m), within and just below the a_p and b_p maxima (Plate 2). During the last 2 days before the hurricane the vertical structure in optical properties associated with particles was observed to change, becoming increasingly more vertically uniform. In the days following the hurricane passage the highest b_p and a_p values were both found in the bottom half of the water column, and

Table 1. Optical, Physical, and Chemical Properties Observed in Three Depth Ranges During Summer 1996 and Spring 1997 at 40°30 N 70°30´W[a].

	Summer			Spring		
	0-20 m	20-40 m	40-65 m	0-20 m	20-40 m	40-65 m
a_p(440)-ac9	0.044 (0.010)	0.076 (0.024)	0.064 (0.036)	0.087 (0.017)	0.064 (0.007)	0.056 (0.008)
a_{ph}(440)-spec	0.042 (0.011)	0.042 (0.024)	0.014 (0.007)	0.072 (0.017)	0.040 (0.011)	0.014 (0.006)
a_d(440)-spec	0.017 (0.006)	0.031 (0.016)	0.068 (0.037)	0.024 (0.006)	0.026 (0.006)	0.030 (0.006)
a_{CDOM}(440)	0.060 (0.007)	0.078 (0.005)	0.081 (0.005)	0.065 (0.006)	0.063 (0.003)	0.067 (0.004)
b_p(440)	0.312 (0.097)	0.325 (0.124)	0.425 (0.298)	0.363 (0.081)	0.232 (0.044)	0.244 (0.050)
K_d(443)	0.133 (0.022)	0.186 (0.030)	0.148 (0.034)	0.192 (0.021)	0.157 (0.010)	0.140 (0.013)
R_{rs}(443), sr^{-1}	0.0029 (0.0004)			0.0021 (0.0004)		
Chl *a*, mg m^{-3}	0.48 (0.15)	0.80 (0.41)	0.17 (0.11)	1.83 (0.56)	1.17 (0.34)	0.56 (0.31)
Phaeo, mg m^{-3}	0.19 (0.08)	0.51 (0.23)	0.27 (0.14)	0.96 (0.38)	0.67 (0.22)	0.34 (0.13)
NO_3+NO_2, µM	0.09 (0.12)	4.60 (5.65)	4.09 (8.01)	2.46 (1.28)	5.15 (2.11)	7.12 (3.17)
PO_4, µM	0.30 (0.13)	4.69 (5.57)	3.85 (8.10)	1.30 (0.96)	4.43 (2.92)	5.63 (4.81)
SiO_4, µM	ND	ND	ND	2.42 (0.87)	5.06 (2.13)	7.17 (3.16)
Temperature, °C	15.74 (1.17)	10.91 (0.88)	9.29 (1.07)	7.63 (0.66)	6.94 (0.49)	6.05 (0.10)
Salinity, psu	31.84 (0.09)	32.12 (0.09)	32.31 (0.11)	32.21 (0.10)	32.30 (0.04)	32.36 (0.03)
σ_t, kg m^{-3}	23.35 (0.30)	24.55 (0.22)	24.96 (.27)	25.13 (0.16)	25.30 (0.08)	25.46 (0.03)

[a]Values indicated are means (standard deviations) for the sampling periods shown in Plates 1-4, and reflect global values determined after first computing means for each depth range on individual sampling casts. Note that vertical and temporal differences in sampling for the ac-9 and spectrophotometric (spec) absorption measurements (see section 2) likely contributed to some of the differences observed between the two methods, especially near the bottom of the water column. Average K_d(443) values for the shallowest depth range were based on observations in the top 15 m as in Figure 5 and for the deepest range, only observations between 40 and 50 m were included since E_d(443) was often too low for reliable detection below 50 m. R_{rs} values reported under 0-20 m were calculated on the basis of water-leaving radiance as described in the text. Unless otherwise noted, units are m^{-1}. ND indicates quantities not determined.

b_p(440):a_p(440) was very low in the surface layer (mean ± s.d. = 2.8 ± 0.7 for <20 m; after September 3 in Plate 2). Throughout the sampling period, CDOM absorption (a_{CDOM}) was systematically higher below the mixed layer but varied overall only between ~0.05 and 0.09 m^{-1} at 440 nm (Plate 2b and Table 1).

3.1.2. Spring 1997. In April and May the observed range of salinity values was nearly the same as summer (~31.8-32.5 psu), but water temperatures were much lower (~6-9°C). Vertical gradients in both properties were also low leading to weaker stratification compared to the previous summer. Stratification did increase with time, however, over the 3 week sampling period (Plate 3a) as surface waters warmed and freshened [*Gardner et al.*, this issue]. Vertical structure in Chl *a* consistently showed highest concentrations (ranging from ~1 to 4 mg m^{-3}) in the upper 25 m, with a rapid decline below the mixed layer (Plate 3b). Temporally, concentrations were highly variable with a series of 1-2 day patches in time evident during the first half of the sampling period and a more sustained apparent bloom occurring later (after May 4). Nitrate plus nitrite concentrations were relatively constant with depth, ranging from ~2 to 5 µM early in the sampling period and then decreasing in surface waters during the bloom period, although concentrations never fell below 0.45 µM (Plate 3c). Nitrite concentrations, which covaried with nitrate, were an average of 0.13 µM and did not exceed 0.23 µM. Diffuse attenuation coefficients showed a consistent vertical pattern with highest values in the surface layer throughout the sampling period, secondary peaks near the bottom, and intermittent mid-water column minima (Plate 3d). Surface values increased on May 4 coincident with the onset of the Chl *a* increase.

Maxima in absorption and scattering coefficients occurred intermittently in the top 20 m of the water column and were always associated with particulate material (Plate 4). Average a_p values at 440 nm increased by >40% in the upper 20 m after May 4, with highest values (>0.13 m^{-1}) observed on May 5; b_p values were also highest (>0.5 m^{-1} at 440 nm) in the surface layer at this time. Both a_p and b_p values generally exhibited mid-water column minima near 40 m. In contrast to summer conditions, b_p(440):a_p(440) was relatively low and constant in depth and time (overall mean ± s.d. = 4.1 ± 0.8; compare Plates 2d and 4d). While dissolved material contributed significantly to absorption in the blue-to-green region of the spectrum, a_{CDOM} was even less variable (~0.06–0.07 m^{-1} at 440 nm) with depth and time than observed in the preceding summer (compare Plates 2b and 4b; Table 1).

3.2. Spectral Variations

Differences in the spectral shape of some optical properties were evident both within and between the two cruises. Spectral differences between the cruises were most evident in reflectance measurements. Surface waters were generally darker and greener in spring, exemplified by R_{rs} values that were lower at blue wavelengths but slightly higher at 555 nm compared to the summer (Figure 1a and Table 2; mean R_{rs}(443):R_{rs}(555) = 1.62 for summer and 0.90 for spring). At blue and green wavelengths, mean K_d values in surface waters (<15 m) were higher in the spring, and there was a small but significant spectral shift toward enhanced blue relative to green attenuation compared to summer (Figure 1b; mean K_d(443):K_d(555) = 1.20 for summer and 1.43 for spring). The mean spectral shift in K_d between the seasons was significantly less than that observed for R_{rs} ($p \ll 0.001$ for ratios of

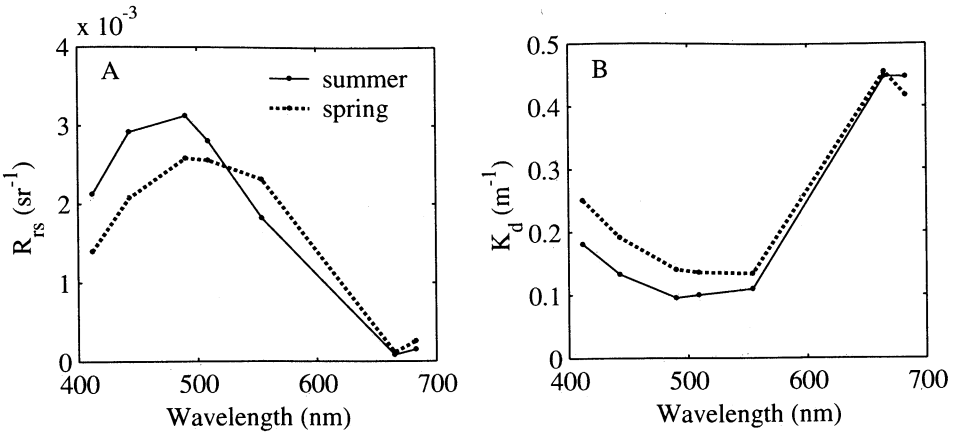

Figure 1. Mean spectra of (a) R_{rs} and (b) near-surface (<15 m) K_d for summer 1996 and spring 1997. The legend in Figure 1a applies to both panels.

443 to 555). For both cruises the K_d values at 665 and 683 nm are near those predicted for pure seawater [*Morel*, 1988] instead of being higher, most likely because of the influence of Chl *a* fluorescence and possibly Raman scattering at these wavelengths [*Berwald et al.*, 1998; *Morrison*, 1999]. Chl *a* fluorescence is also evident in R_{rs} as a peak at 683 nm (Figure 1a), as expected [e.g., *Roesler and Perry*, 1995].

Spectral variability in inherent optical properties was most apparent in the particulate pool and as a function of depth. Average absorption spectra observed for the surface layer (<20 m), mid-water column (20-40 m), and bottom layer (>40 m) emphasize that variations in magnitude or spectral shape of a_{CDOM} were not as great as those observed for a_p (Figures 2a, 2c, and 2e and Tables 1 and 2). At 440 nm, for instance, overall variance for a_p was significantly higher than that for a_{CDOM} in both seasons (t test: p <<0.001 in both cases). On the basis of either spectrophotometric analysis of discrete samples or in situ ac-9 measurements, average surface layer a_p signals varied in magnitude between spring and summer (Figure 2a and Table 1) more than in spectral shape (Figures 3a and 3b and Table 2). In the mid-water column, average absorption spectra were similar in both magnitude and shape between the two seasons (Figures 3c and 3d and Tables 1 and 2), although standard deviations were higher in summer (e.g., 0.024 versus 0.011 m^{-1} for a_{ph} and 0.016 versus 0.006 m^{-1} for a_d at 440 nm, Table 1). In the bottom layer, average a_p values based on discrete measurements were higher in summer and lower in spring compared to the ac-9 measurements (Figure 2e and Table 1). These discrepancies may be due partly to depth and time differences in sampling but also to uncertainties in path length amplification effects for the glass fiber filters and other potential problems such as clogging, inefficient filtration, or particle destruction during ac-9 measurements. Regardless of method, however, a_p exhibited different

Table 2. Selected Spectral Ratios for Various Optical Properties Observed in Three Depth Ranges During Summer 1996 and Spring 1997 at 40°30′N 70°30′W[a].

	Summer			Spring		
	0-20 m	20-40 m	40-65 m	0-20 m	20-40 m	40-65 m
a_p(412:488)-ac9	1.62 (0.40)	1.49 (0.30)	1.89 (0.45)	1.32 (0.08)	1.44 (0.11)	1.81 (0.19)
a_{ph}(412:488)-sp	1.07 (0.05)	1.00 (0.07)	1.17 (0.24)	1.06 (0.05)	1.02 (0.05)	1.10 (0.16)
a_d(412:488)-sp	2.13 (0.21)	2.07 (0.20)	2.20 (0.09)	2.08 (0.17)	2.09 (0.11)	2.27 (0.12)
a_{CDOM}(412:488)	3.66 (0.35)	3.57 (0.32)	3.59 (0.35)	3.96 (0.25)	3.96 (0.18)	3.97 (0.16)
b_p(412:488)	1.00 (0.05)	1.07 (0.05)	1.08 (0.05)	1.06 (0.04)	1.07 (0.03)	1.09 (0.03)
a_p(440:676)-ac9	2.47 (0.41)	2.53 (0.55)	4.44 (1.87)	2.46 (0.24)	2.71 (0.27)	3.70 (0.60)
a_{ph}(440:676)-sp	2.17 (0.36)	1.64 (0.17)	1.84 (0.53)	1.69 (0.11)	1.56 (0.09)	1.72 (0.29)
a_d(440:676)-sp	7.08 (3.06)	5.78 (1.07)	6.29 (0.65)	6.17 (1.22)	5.57 (0.94)	5.99 (1.11)
b_p(440:676)	1.21 (0.12)	1.18 (0.11)	1.18 (0.07)	1.17 (0.14)	1.25 (0.05)	1.30 (0.05)
K_d(412:490)	1.89 (0.10)	1.70 (0.24)	ND	1.79 (0.07)	1.93 (0.07)	ND
K_d(443:554)	1.20 (0.11)	1.34 (0.10)	1.10 (0.14)	1.43 (0.07)	1.27 (0.04)	1.19 (0.04)
R_{rs}(412:490)	0.68 (0.06)			0.54 (0.06)		
R_{rs}(443:554)	1.62 (0.25)			0.90 (0.13)		

[a]Values indicated are means (standard deviations) for the sampling periods shown in Plates 1-4 and reflect global values determined after first computing means for each depth range on individual sampling casts. As in Table 1, the spectral ratios for K_d are presented for 0-15 m in place of 0-20 m, and R_{rs} ratios are based on water-leaving radiance; in addition, E_d(412) and E_d(443) were too low below 40 and 50 m, respectively, to allow K_d to be reliably estimated. ND indicates quantities not determined.

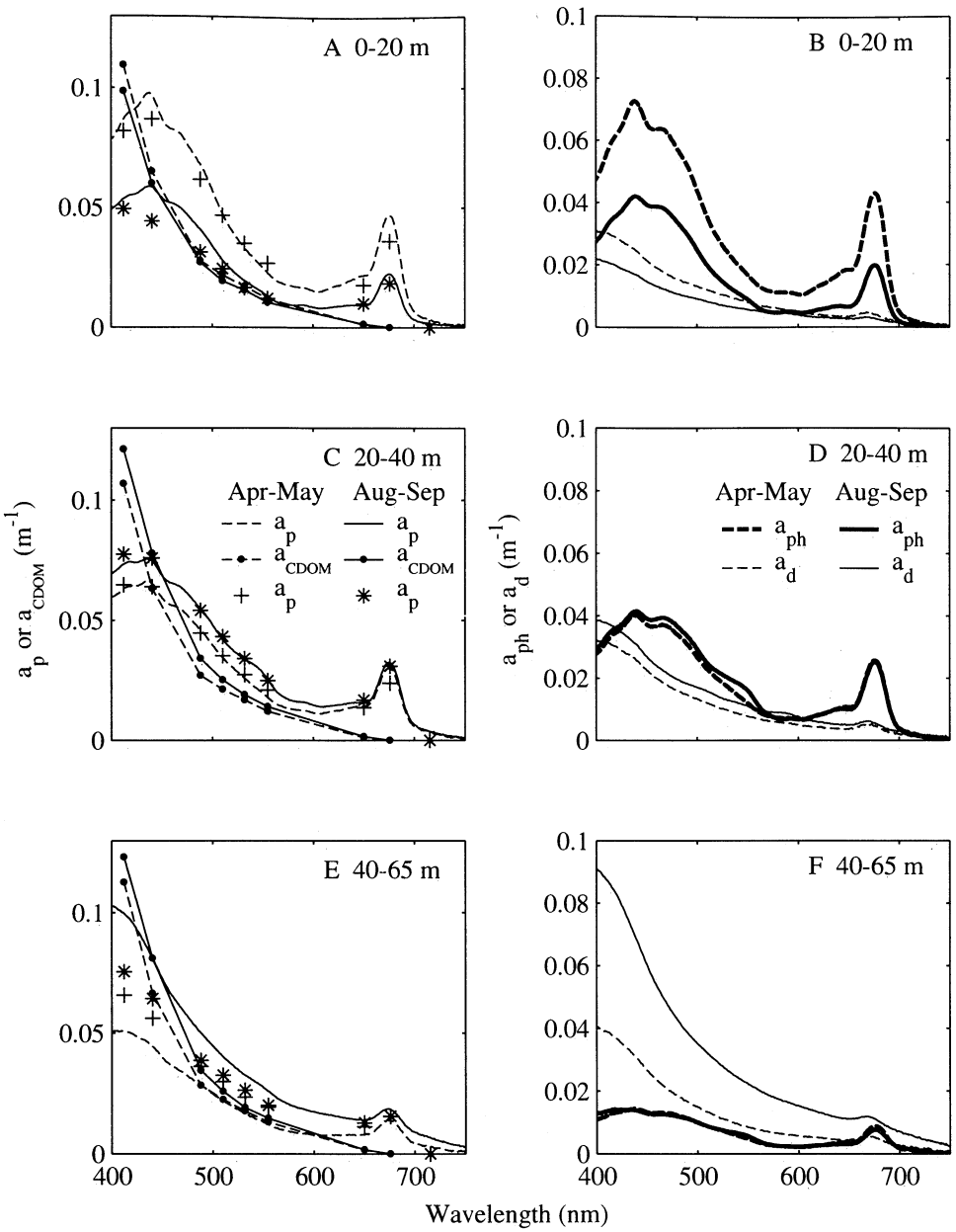

Figure 2. Mean absorption spectra for different constituents in upper (<20 m), middle (20–40 m), and bottom (>45 m) layers of the water column during summer 1996 and spring 1997. CDOM absorption spectra were derived from in situ ac-9 measurements (dots with lines); particulate absorption from both ac-9 measurements (asterisks and pluses) and spectrophotometric analysis of discrete water samples (lines only) are indicated (Figures 2a, 2c, and 2e). Mean phytoplankton and detrital absorption spectra were measured spectrophotometrically on discrete water samples (Figures 2b, 2d, and 2f). The legends in Figures 2c and 2d apply to all left and all right panels, respectively.

spectral shape in the near-bottom waters compared to other depths during both seasons (Figures 2, 3a, and 3b and Table 2). This appears to be due primarily to higher a_d signals relative to a_{ph} rather than to major shifts in the spectral shapes of a_{ph} or a_d (Figures 2 and 3 and Tables 1 and 2). In the bottom layer, mean a_d signals were much higher in summer compared to spring (Figure 2f and Table 1). This result was less apparent in the period before August 29 when a_d at 440 nm averaged 33% lower than the global mean for the bottom layer. For particle scattering coefficients, although the magnitude varied widely (see Plates 2c and 4c), mean normalized spectra were <10% different between cruises and among depth layers (Figure 4 and Table 2).

4. Discussion

Vertical and temporal variability in both the physical and optical properties of the water column were observed at this coastal site. In general, for optical properties the magnitudes of vertical and temporal variability were similar. The relationships between physical and optical variability differed, however, indicative of different forcing processes for vertical

and temporal changes. From the relationships between various optical properties it is possible to gain some insights into these processes.

4.1. The Importance of Particles

Observed vertical and temporal changes in the magnitude of water column optical properties such as K_d were primarily due to particles. During the stratified period in late summer, vertical profiles of $K_d(440)$ typically showed mid-water column maxima (Plate 1d) at the same depths as peaks in $a_p(440)$ and $b_p(440)$ (Plates 2a and 2c). Similarly, after the passage of Hurricane Edouard the strong $K_d(440)$ maximum evident in the bottom layer was associated with the highest values of a_p and b_p observed during the entire sampling period. In the spring, $K_d(440)$, $a_p(440)$, and $b_p(440)$ were all highest in the top 20-30 m, particularly after May 4. During summer, meas-

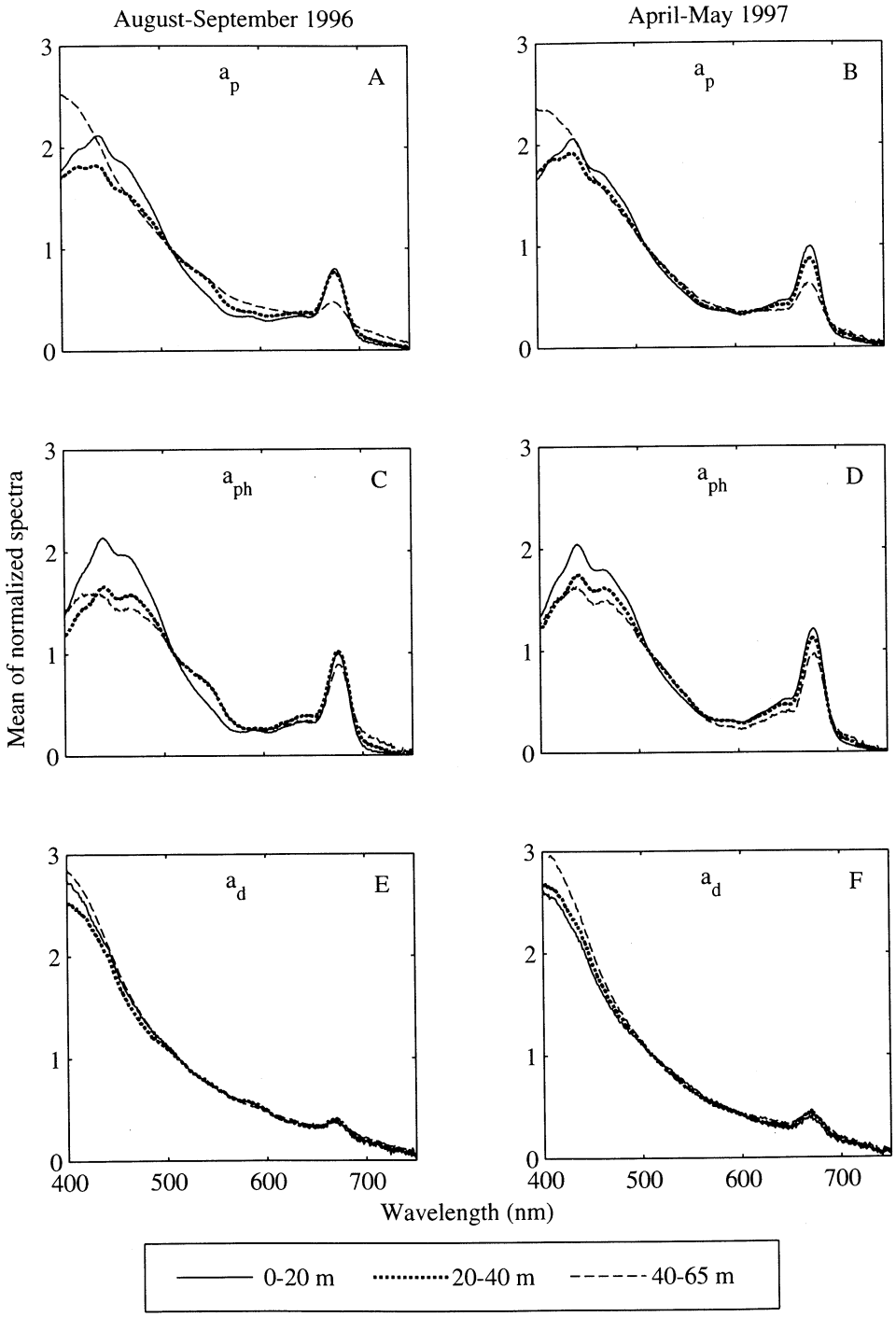

Figure 3. Differences in spectral shape among depth layers and between seasons indicated by means of absorption spectra normalized to 510 nm for total particles and for the phytoplankton and detrital components: (a) a_p for summer, (b) a_p for spring, (c) a_{ph} for summer, (d) a_{ph} for spring, E) a_d for summer, and F) a_d for spring.

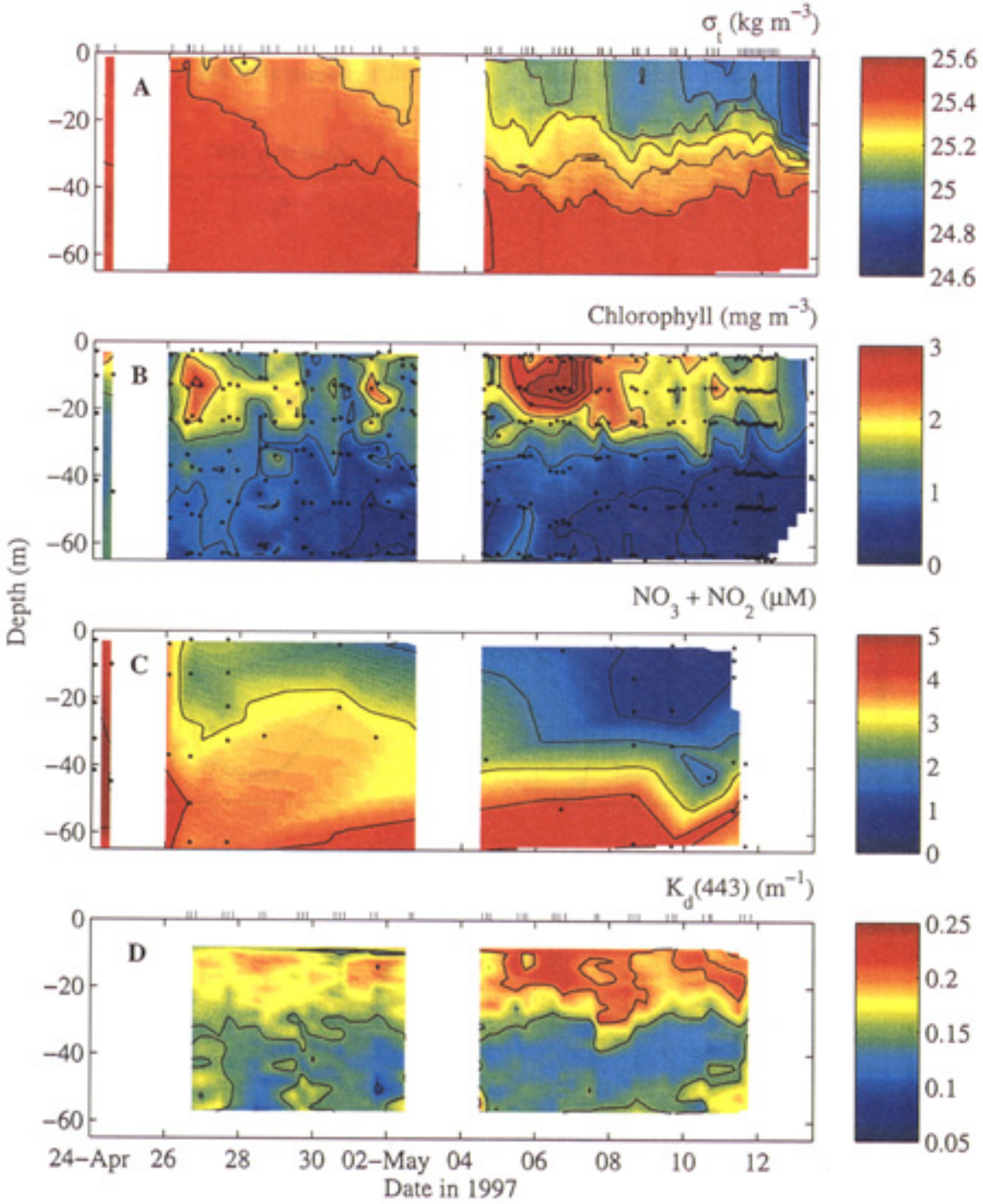

Plate 3. As in Plate 1, but for the spring 1997 sampling period. Density values are from measurements made with the ship's SeaBird CTD during rosette casts to collect discrete water samples. Note difference in color scale from Plate 1. Contours (black lines) are drawn at intervals of 0.1, 0.5, 1, and 0.05 in Plate 3a, 3b, 3c, and 3d, respectively.

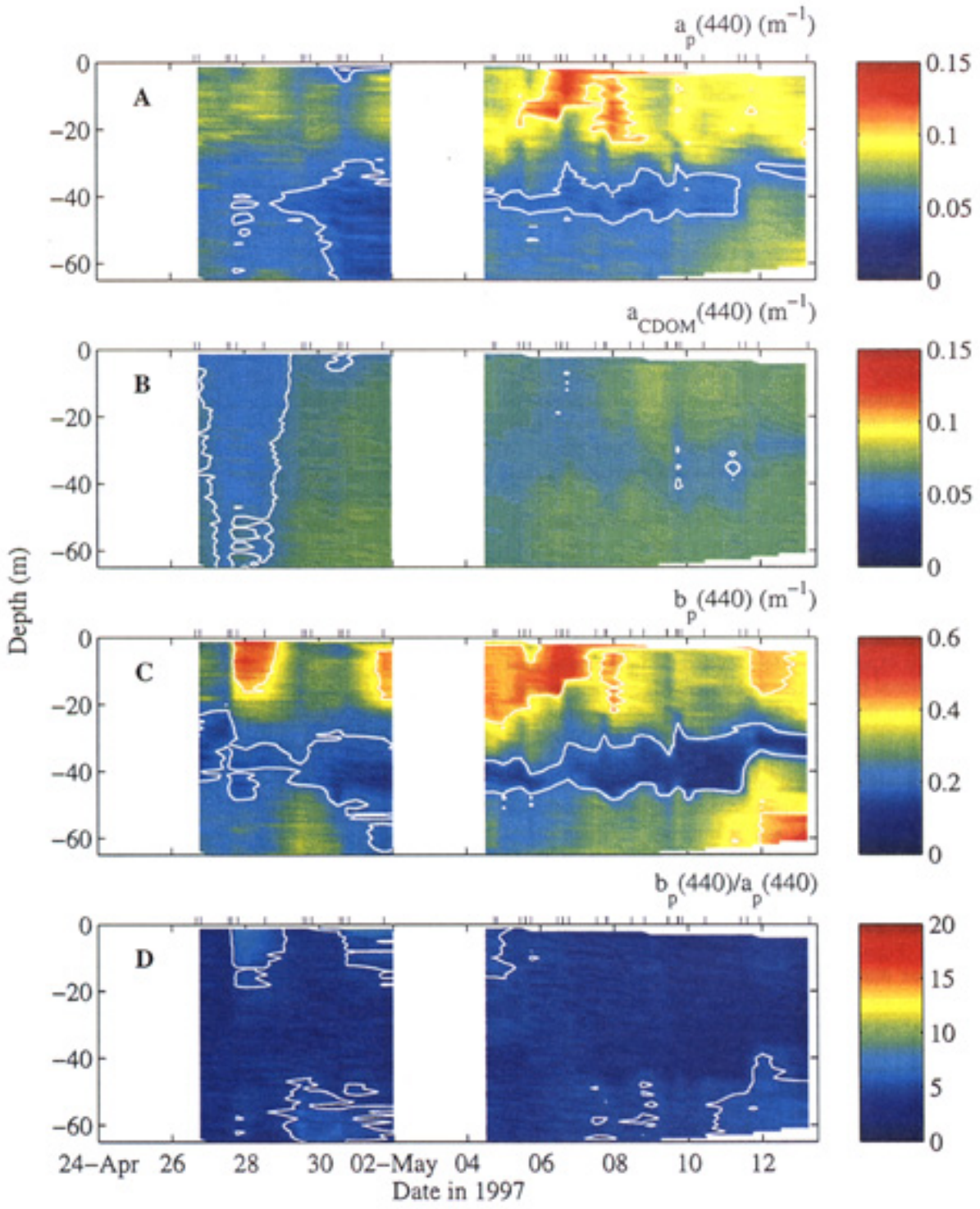

Plate 4. As in Plate 2, but for the same period shown in Plate 3. Color scale and contour levels are the same as for Plate 2.

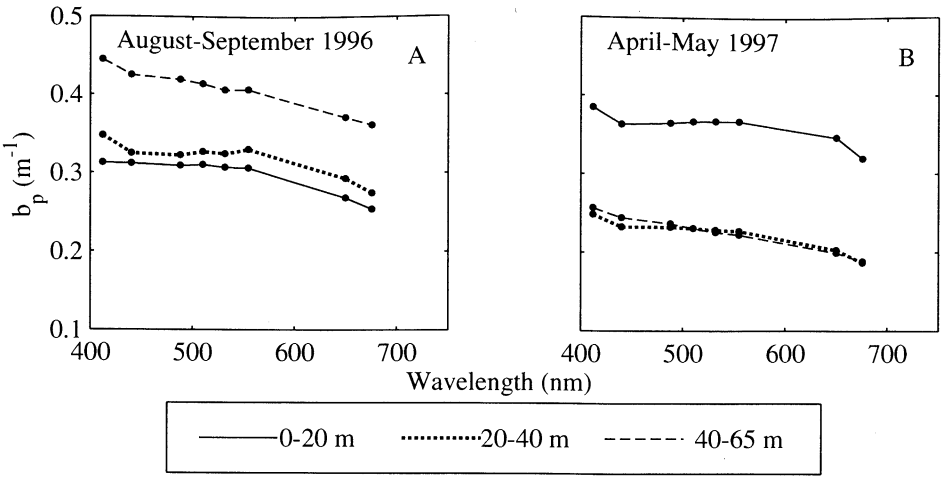

Figure 4. Mean scattering spectra for particulate material in the upper (<20 m), middle (20–40 m), and bottom (>45 m) layers of the water column during (a) summer 1996 and (b) spring 1997.

urable variability in a_{CDOM} was observed, with low near-surface values most likely due to photo-oxidation under stratified conditions and with intermittent elevated values near the bottom due to resuspension events [*Boss et al.*, this issue]. At most wavelengths, however, these changes were smaller than those in a_p.

While particulate material was observed to dominate variability, dissolved material was optically important during both seasons. This importance increased with decreasing wavelength because of the characteristic exponential spectral shape for absorption by CDOM [*Bricaud et al.*, 1981; *Carder et al.*, 1989; *Roesler et al.*, 1989]. As suggested by *Siegel et al.* [1995], this is expected to affect K_d, and the influence of total nonalgal material (particulate and dissolved) can be generally characterized by the ratio of K_d at 410 nm to K_d at 490 nm. In surface waters we observed typical $K_d(412):K_d(490)$ values of 1.9 and 1.8 in the summer and spring, respectively, indicative of a relatively high nonalgal contribution and little seasonality. In contrast, for the Sargasso Sea, highest mixed layer values observed are ~1.3, and seasonality has been documented, with typically lower values in summer [*Siegel et al.*, 1995; *Siegel and Michaels*, 1996]. The relative importance of CDOM can be further explored by examining the relationships between absorption coefficients and K_d at different wavelengths (Figure 5). To first order, K_d and the absorption coefficient are directly related [e.g., Kirk, 1994], and to the extent that variations in the average value of cosine of the zenith angle weighted over the underwater radiance field are small, the relative influence of particles and dissolved material can be evaluated by simple correlation analysis over all observations. For the blue and green wavelengths the relationship between K_d and a_p consistently exhibited a higher slope than that with a_{CDOM}, emphasizing the important role of particles in K_d variability. High correlation coefficients (r^2 = 0.45-0.78) also support the conclusion that a_p is consistently a dominant source of variance in K_d (Figure 5). Especially in the spring, the overall range of observed a_{CDOM} values was low compared to a_p, but a_{CDOM} signals were significant in magnitude in both seasons. This is especially evident at 412 nm where a_{CDOM} consistently exceeded a_p (Figures 5a and 5b). Even at 443 nm, a_{CDOM} was often of comparable magnitude to a_p (see Table 1) and thus contributed significantly to the magnitude of K_d, especially when a_p was relatively low such as in the surface layer during summer stratification. During summer the somewhat larger range of a_{CDOM} values and the higher covariance with K_d are associated with the vertical gradient in a_{CDOM} observed in the upper 40 m of the water column before the hurricane (Plate 2b).

These conclusions about the significance of a_{CDOM} magnitude are consistent with previous studies of midshelf surface waters in the North Atlantic, while the low level of temporal and vertical variability observed contrasts with reports for horizontal variability. Absorption by CDOM in both seasons was similar to values reported by *Nelson and Guarda* [1995] for surface waters at midshelf locations in the South Atlantic Bight (SAB) during summer 1992 and by *DeGrandpre et al.* [1996] for midshelf surface waters of the Mid-Atlantic Bight (MAB) in summer and fall 1994. In both of these studies, a_{CDOM} values were observed to be comparable to or to exceed a_p values at blue wavelengths. Much higher values (approximately twofold to tenfold) of a_{CDOM} were encountered, however, on the midshelf of the SAB in spring (April) and on the inner shelves of the SAB and MAB in all seasons, correlated with water of lower salinity. Higher values of a_{CDOM} inshore and a cross-shelf inverse salinity dependence were also evident during CMO [Boss et al., this issue]. These observations emphasize that the low level of variability in a_{CDOM} compared to a_p found at the CMO central site for summer 1996 and spring 1997 cannot be generalized to larger horizontal scales or necessarily to longer time scales. Seasonal and interannual changes in land runoff may be important in determining CDOM variability [e.g., *Nelson and Guarda*, 1995], as are processes contributing to conservative mixing across the shelf.

4.2. Different Particle Types

Since local variability in inherent and apparent optical properties on timescales from days to weeks was dominated by changes in particle absorption and scattering, the nature of this particulate material deserves further investigation. Important particles may include phytoplankton of varying pigment composition and cell size, detrital material, heterotrophic microorganisms including bacteria and protozoa, various

minerals with or without organic coating, and composites or aggregates of any of these. Spectral absorption characteristics provide some insight into the importance of major types of particles: phytoplankton and a relatively poorly characterized class of "detrital" material. Using present methods for absorption analysis, the detrital or nonalgal fraction is operationally defined as material with chromophores that are not soluble in methanol [*Kishino et al.*, 1985] and may include any of the particle types mentioned above.

4.2.1. Particle absorption. Most of the large changes observed in the magnitude of a_p were due to the phytoplankton fraction, which, as expected, varied with Chl *a* concentration (Figure 6). This was true for temporal and vertical changes evident in both seasons, with the exception of conditions in bottom waters highly influenced by resuspension during summer (see below). Similar to the case for a_{CDOM}, the relative significance of a_d increased with decreasing wavelength; however, in spring even at 412 nm the overall range of observed a_d values was smaller than that found for a_{ph} (Figure 6). In addition, a_d values were usually lower than a_{CDOM} (Figure 2 and Table 1) and thus less important in determining the magnitude and spectral shape of K_d discussed above. For particles the shapes of mean a_p spectra were consistent with phytoplankton dominance in the upper water column during

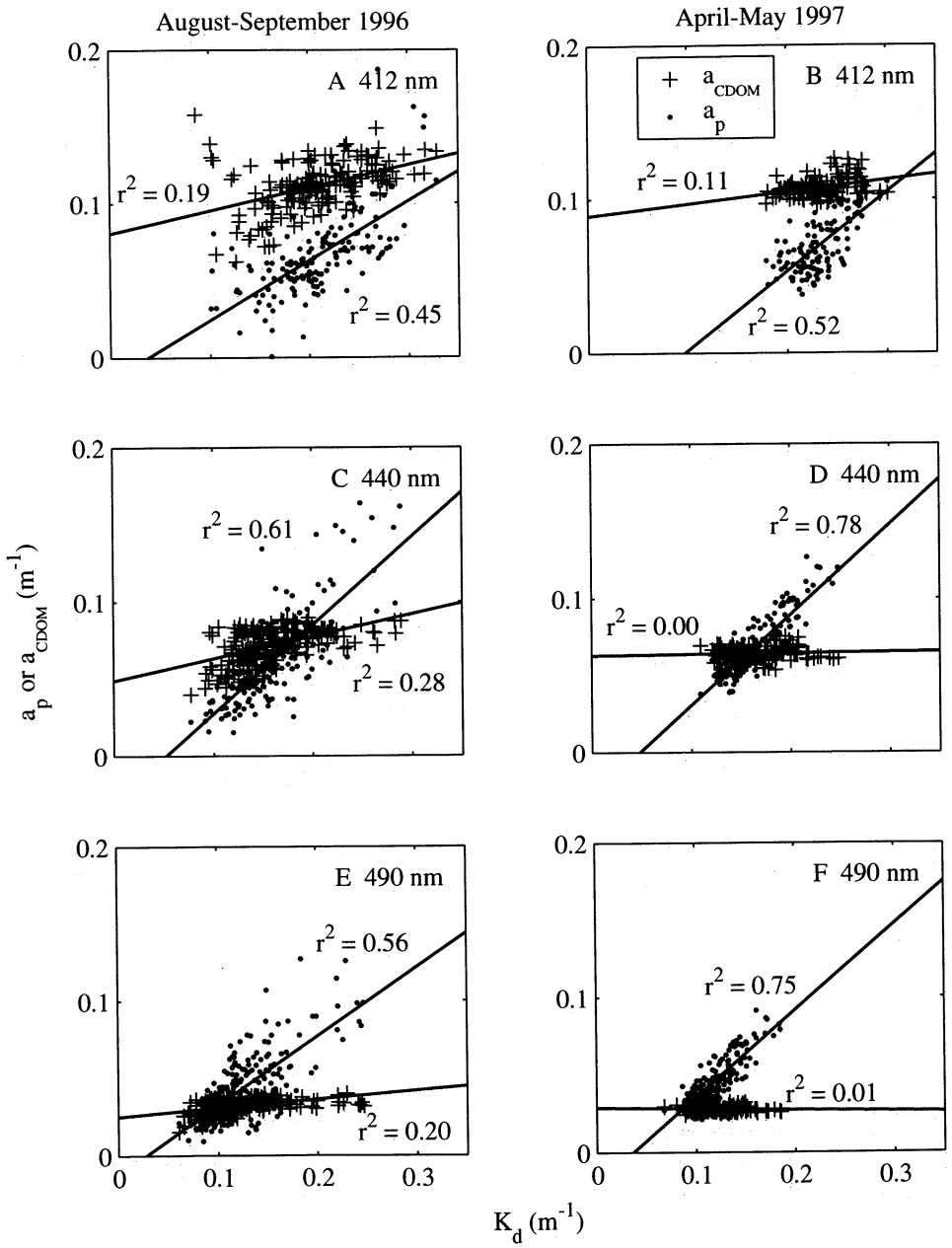

Figure 5. Scatterplots of a_p and a_{CDOM} versus K_d at (a) and (b) 412, (c) and (d) 440 (or 443), and (e) and (f) 490 (or 488) nm for all depths and times sampled in summer 1996 and spring 1997. Absorption values were derived from ac-9 profiles conducted within 2 hours of the radiometer casts. Data points represent averages over ten 1 m bins. Because of sensitivity limits of the radiometer, no observations below 40 and 50 m were included for 412 and 440 nm, respectively. The proportion of variation explained by simple linear regression r^2 is indicated for each case. The legend in Figure 5b applies to all panels.

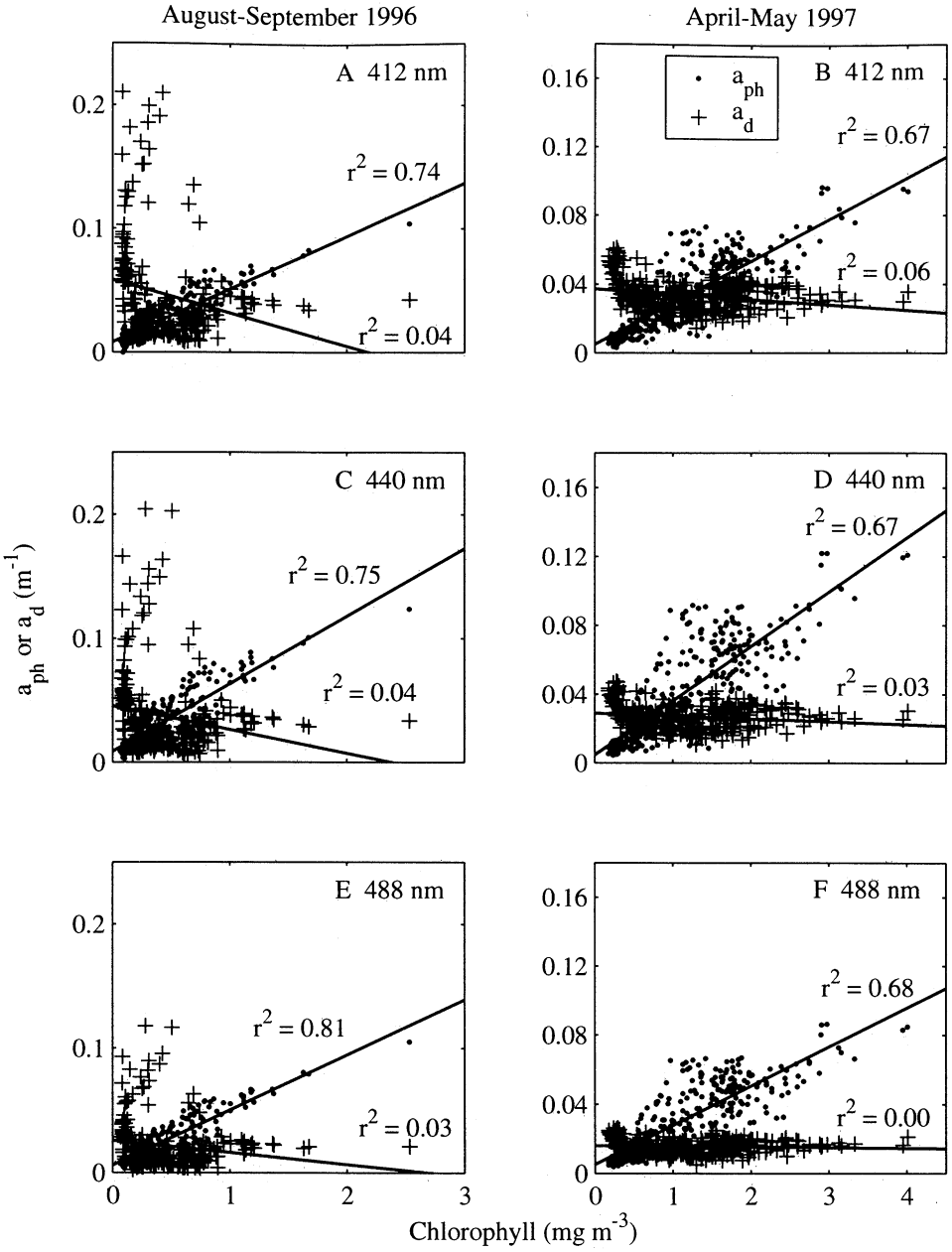

Figure 6. Scatterplots of a_{ph} and a_d at (a) and (b) 412, (c) and (d) 440, and (e) and (f) 488 nm versus Chl *a* concentration for all depths and times sampled in summer 1996 and spring 1997. Absorption values and Chl *a* concentrations were measured in the laboratory on discrete water samples from the same CTD/rosette casts. The proportion of variation explained by simple linear regression r^2 is indicated for each case. The legend in Figure 6b applies to all panels.

both seasons (Figure 2 and Table 2). This contrasts with results for midshelf surface waters observed by *Nelson and Guarda* [1995], who found that a_d significance increased enough to mask the blue-green phytoplankton absorption maximum in spring compared to summer. An overall range in a_{ph} exceeding that observed for a_d has been frequently observed in other coastal systems [*Roesler et al.*, 1989; *Cleveland*, 1995; *Sosik and Mitchell*, 1995], however, and relatively high a_d observed during the Nelson and Guarda study occurred at the same time as even larger increases in a_{CDOM}. These results are consistent with nonalgal particulate material playing a relatively small role in regulating the optical properties of most coastal waters.

The notable exception to the conclusion that phytoplankton dominated changes in a_p was the occurrence of some high a_d values in low Chl *a* waters during the summer (Figures 6a, 6c, and 6e). These waters with elevated a_d correspond to posthurricane observations and some near-bottom samples before the hurricane. The high values of a_d relative to a_{ph} in these samples are associated with resuspension of bottom sediments, which occurred during the last week of sampling and periodically before. As evident from the low values of a_d consistently observed in spring even for low Chl *a* waters, resuspension of a_d-dominated material into the bottom layer was more important in summer (Figures 2e and 6). This resuspension occurred as a result of long-period swell associated with Hur-

ricane Edouard and possibly the greater internal wave activity observed when the water column was highly stratified [*Dickey et al.*, 1998; *Chang et al.*, this issue; *Gardner et al.*, this issue]. While these events may also have resulted in increases in a_{CDOM} in bottom waters [*Boss et al.*, this issue], these changes were small relative to those associated with particles (Plate 2). The importance of a_d in bottom waters is also supported by variations in the shape of the a_p spectrum. These variations were primarily due to changes in the relative contributions of phytoplankton and detrital absorption (Figures 2 and 3 and Table 2). During spring the shift toward a detrital a_p spectrum in the bottom layer resulted from a decrease in a_{ph} relative to mid-water column values; a_d signals remained relatively constant. While a_{ph} was also low in bottom waters in summer, the average magnitude of a_d was higher than in the upper water column, and this was the primary reason for the spectral change in a_p.

In addition to shifts in the relative magnitudes of a_{ph} and a_d, some spectral variations within the particle types also occurred, contributing to overall variability in a_p. For a_{ph}, relatively small but systematic differences between the two seasons in the shape of mean spectra for the upper water column (Table 2) suggest that there were optically important differences between the phytoplankton cells present in summer and spring. In the surface layer, the ratio of the blue to the red maximum in a_{ph} (~440 and 675 nm) was usually >2.0 (mean 2.3) prior to the hurricane, while in spring, values never exceeded 2.0 (mean 1.7). As described by *Sosik and Mitchell* [1995] for spatial variations of this ratio in California coastal waters, this difference is consistent with a smaller-sized, nutrient-limited, and relatively high-light-acclimated phytoplankton assemblage in summer surface waters compared to spring. In summer, surface nitrate concentrations were depleted; the mixed layer was generally shallower, leading to higher average light exposure for cells in the upper water column; and flow cytometric analysis during CMO sampling has documented a greater abundance of picoplankton (*Synechococcus* sp.) [*Sosik et al.*, 1998]. As discussed by *Yentsch and Phinney* [1989], these types of ecological and environmental changes are expected to influence light absorption by particles.

Differences in particle properties for near-bottom waters were also evident in spectral variations in absorption. During the summer, bottom layer a_{ph} spectra exhibited a shift of the blue absorption maximum toward lower wavelengths (Figure 3c), indicating that degraded forms of Chl *a* probably contributed significantly to methanol soluble material in these waters. This suggests that the operationally defined "phytoplankton" absorption (that associated with methanol soluble pigments) in these waters had significant contributions from dead cells and/or fecal material from herbivores. This type of artifact associated with separating phytoplankton and detrital contributions to optical properties can be avoided with individual particle techniques such as microphotometry [*Iturriaga and Siegel*, 1989; *Iturriaga et al.*, 1991], although this approach has its own limitations associated with sample analysis time and minimum particle size. A combination of individual particle techniques and complementary but less detailed bulk measurements may be required to gain further insights into optical characteristics of detrital material.

4.2.2. Particle scattering. On the basis of the vertical and temporal variations in absorption properties we can infer that the dominant types of particles contributing to scattering also varied. High a_p signals associated with phytoplankton in the surface layer during spring and mid-water column during summer consistently coincided with high b_p (Plates 2 and 4), suggesting that phytoplankton and other particles that covary with phytoplankton contributed to these scattering maxima. As suggested by *Stramski and Kiefer* [1991], heterotrophic bacteria, cyanobacteria, and ultrananoplankton (2-8 μm) may have been the most significant contributors. Comparison of a_p and b_p magnitudes suggests that significant changes in the relative importance of different particle types and/or particle properties occurred in the upper water column. Lowest b_p to a_p ratios were observed mid-water column during summer, and highest ratios were found in surface waters during summer (Plates 2d). These patterns are at least partially due to photoacclimation in the phytoplankton [*Sosik et al.*, 1998] consistent with laboratory studies suggesting that absorption per cell should be higher under the low light levels below the mixed layer [e.g., *Dubinsky et al.*, 1986; *Mitchell and Kiefer*, 1988; *Stramski and Morel*, 1990]. In summer surface waters, high light levels, combined with high cyanobacteria abundance contributing to a small particle size distribution, were probable factors causing elevated b_p:a_p. The very high values of $b_p(440)$:$a_p(440)$ often observed in the top 10-15 m during summer (Plate 2d), however, cannot be explained solely on the basis of absorption and scattering by phytoplankton. Estimates based on experimental work and theoretical considerations of b_p:a_p for a wide variety of phytoplankton types (including picoplankton) do not exceed ~5 or 6 at 440 nm [*Bricaud et al.*, 1983, 1988; *Stramski and Morel*, 1990; *Stramski and Mobley*, 1997]. The highest values observed in summer are consistent with a significant scattering signal due to weakly absorbing particles such as heterotrophic bacteria, which can have b_p:a_p ~20 at 440 nm according to *Stramski and Mobley* [1997].

In contrast to the upper water column, the elevated b_p signals observed in waters below 50 m are unlikely to be associated with viable phytoplankton cells since a_{ph} signals were quite low (Figure 2). Additionally, as discussed above, it is likely that a_{ph} measured in these waters overestimates absorption by living cells because of inclusion of degraded pigment forms. The characterization of the particles and aggregates present in the bottom boundary layer is discussed elsewhere [e.g., *Hill et al.*, this issue; *Agrawal and Traykovski*, this issue].

4.3. Vertical Variability and Seasonal Differences

During both summer and spring seasons, vertical gradients were observed in the inherent and apparent optical properties of the water column. Most characteristics of the observed vertical distributions for absorption, scattering, and diffuse attenuation coefficients are related to the well-known seasonal cycle of stratification and mixing in this region [see *Chang and Dickey*, this issue], primarily through its effects on phytoplankton. As expected on the basis of the success of pigment-based models for K_d [e.g., *Smith and Baker*, 1978; *Morel*, 1988], for instance, optical property distributions covaried with the Chl *a* distribution. During the stratified summer period, maximum K_d values at blue and green wavelengths occurred in the mid-water column Chl *a* maximum, while in the spring, maxima in K_d were evident in the surface

layer, especially in conjunction with the phytoplankton bloom (Plates 1 and 3 and Table 1).

The patterns we observed in Chl *a* distribution are characteristic of shelf waters in this region, for which seasonal physical and biological variability has been well documented for this study [*Chang and Dickey*, this issue] and for previous studies [*O'Reilly et al.*, 1987; *Walsh et al.*, 1987; *O'Reilly and Zetlin*, 1998]. Typically, the wintertime water column is well mixed, nutrient concentrations are high, and Chl *a* concentrations are low. With the onset of stratification a spring bloom generally occurs in March-April, followed by surface nutrient depletion and highly stratified summer conditions with a pronounced subsurface Chl *a* maximum. As described by *Ryan et al.* [1999a], during the transition between the spring bloom and summer stratification a band of enhanced surface Chl *a* concentration often develops along the shelfbreak (in the vicinity of the 100 m isobath). This feature is an apparent response to along-isopycnal upwelling of nutrients in deep shelf waters forced by meanders of the shelfbreak front [*Marra et al.*, 1990; *Ryan et al.*, 1999b].

During our sampling these general seasonal patterns were evident and had a major influence on optical variability. In the highly stratified summer period, absorption and scattering by particles were low in the surface waters, where phytoplankton were exposed to high-light and low-nutrient conditions. The mid-water column maxima in optical properties coincided with the high levels of phytoplankton pigment present in response to low light levels and the depth of the nitracline (Plates 1 and 3). During spring 1997, satellite ocean color imagery from May 2 and 5 reveals that our sampling site was on the edge of a band of high-Chl *a* water at the shelfbreak, with lower pigment concentrations present over the rest of the mid-shelf [*Ryan et al.*, 1999b]. These observations suggest that the phytoplankton bloom and associated changes in absorption and scattering, during our sampling in early May (Plates 3 and 4), were fueled by nutrients upwelled in the vicinity of the shelfbreak. The combination of available nutrients and an increase in stratification were critical factors.

The same physical and biological dynamics that control the seasonal differences in vertical distributions of optical properties were also important in determining surface reflectance spectra. In spring, when particulate absorption and scattering were highest near the surface of the water column, R_{rs} values were lower and green-shifted relative to summer (Figure 1a and Tables 1 and 2). During summer, absorption and scattering coefficients were much lower in surface waters coincident with higher R_{rs} magnitude and a higher ratio of blue to green values [e.g., *Gordon et al.*, 1988]. While differences in the magnitude of absorption and scattering in surface waters were important, the smaller spectral difference observed in K_d compared to R_{rs} (Figure 1 and Table 2) suggests that these were not the only factors in the R_{rs} seasonal difference. If backscattering is small and has low wavelength dependence relative to absorption and we assume that reflectance is proportional to b_b:a, then a spectral ratio for R_{rs} should be roughly equal to the inverse of the same ratio for K_d. For the springtime observations of mean spectra the ratios for 443 and 555 differ by <25% ($R_{rs}(443)$:$R_{rs}(555)$ = 0.90; $K_d(555)$:$K_d(443)$ = 0.70), while for summer the difference is almost 50% ($R_{rs}(443)$:$R_{rs}(555)$ = 1.62; $K_d(555)$:$K_d(443)$ = 0.83). This contrast suggests that particle backscattering properties differed between the two seasons; in particular, a steeper inverse wavelength dependence and/or higher backscatttering efficiency as predicted for the smaller particles may have occurred in summer. As discussed above, seasonal differences in the shape of the a_{ph} spectrum and in the ratio of scattering to absorption are also consistent with this hypothesis of an optically important shift in particle size distribution for surface waters. Although their methods only considered phytoplankton smaller and larger than 20 μm, these results are generally consistent with the observations of *O'Reilly and Zetlin* [1998], who documented a seasonal pattern for this region with a shift toward larger cells in spring. As discussed by *Yentsch and Phinney* [1989] and *Chisholm* [1992], this general shift may result from ecological responses of the plankton to nutrient availability.

4.4. Short Term Temporal Variability

On timescales of days to weeks, important temporal variability in both the physical structure of the water column and its optical properties is consistent with effects from a variety of processes including weather, shelfbreak frontal dynamics, phytoplankton growth, and advection. During the summer sampling period, changes that occurred with the passage of Hurricane Edouard were the largest temporal perturbations observed for both inherent and apparent optical properties. There were changes in the magnitude, vertical distribution, and spectral shape of diffuse attenuation, absorption, and scattering that occurred in response to this event. As discussed in section 4.2, the effects of the hurricane on optical properties were a distinct exception to the general observation that changes in the phytoplankton dominated optical variability within and between seasons. In the spring a series of smaller storms with high winds that occurred in late April intermittently deepened the mixed layer and were responsible for some of the observed temporal patchiness in particle signals during this period [*Chang and Dickey*, this issue; *Gardner et al.*, this issue].

The most important change evident during the spring time series was associated with the phytoplankton bloom (Plates 3 and 4). As discussed in section 4.3, this bloom occurred during a period when shelfbreak Chl *a* enhancement was observed near the CMO study site and was probably driven by nutrients from deep shelf waters upwelled near the shelfbreak [*Ryan et al.*, 1999b]. The highly variable spatial distribution of pigment concentration typically observed along the edge of the shelfbreak Chl *a* enhancement, combined with frontal interactions leading to seaward transport of shelf waters, may also be responsible for some of the apparent temporal variability evident in spring. This is supported by the appearance of low-salinity surface water during the last week of sampling.

During summer, there were also apparent temporal changes that may have been influenced by advection. The deepening and intensification of the subsurface maxima in Chl *a* and optical properties evident in late August (Plates 1 and 2), for instance, occurred in conjunction with an intrusion of high-salinity water with different optical properties [*Chang and Dickey*, this issue; *Gardner et al.*, this issue]. Another example of a short-term temporal change most likely associated with water mass advection occurred just prior to the hurricane. Decreases in mid-water column Chl *a* concentration and in the magnitudes of a_p, b_p, and K_d occurred over 2-3 days just before sampling was interrupted by the approach of the storm (Plates 1 and 2). While storm effects (long-period swell) were evident at the site during this time, there were no

substantial perturbations in the density structure or in temperature and salinity [see *Gardner et al.*, this issue] that might indicate vertical mixing was responsible for these decreases. Instead, these changes are most likely the result of advection. Results from spatial surveys are consistent with advection of a particle poor water mass along the shelf during this period (J. Barth, personal communication, 1998). Further evidence of advection is indicated by the nitrate plus nitrite distribution, which shows a rapid deepening of the nitracline after August 29 (Plate 1). Since this was not associated with a similar depression of isopycnals, the deeper nitracline was probably the result of enhanced uptake by phytoplankton cells prior to advection into the study area. If this uptake had occurred locally over a couple of days, it is unlikely that it would have been associated with a decline in Chl *a* concentration. While this was beyond the scope of the CMO experiment, further insight into the sources of important horizontal patchiness requires investigation of biologically mediated processes responsible for particle production and loss such as growth, defecation, grazing, sinking, viral lysis, etc. It may be possible to separate more definitely the importance of local and advective processes on the basis of comparison of apparent temporal changes at the central study site with results from concurrent spatial surveys and moored current meter observations.

5. Conclusion

The New England continental shelf is a complex environment where a variety of physical and biological processes influence spatial and temporal variability in optical properties. Since phytoplankton are often the dominant source of this variability, the processes regulating their distribution and properties are of critical importance. These processes can be both cyclic (e.g., diurnal and seasonal) and episodic (e.g., blooms, storms, and advection) and can vary in duration and spatial extent. Seasonal changes in the stratification of the water column are particularly important not only because they play a major role in regulating vertical phytoplankton distributions and conditions for growth but also because the degree of stratification often determines which other types of physical forcing may be acting. Characterization of physical processes is important; however, new insights into controls on optical variability on the continental shelf will also come from a better understanding of biological responses in the plankton including changes in production, trophic interactions, and community composition.

Notation

a_{CDOM} absorption coefficient for dissolved material, m^{-1}.
a_d absorption coefficient for detrital or nonpigmented particulate material, m^{-1}.
a_p absorption coefficient for particulate material, m^{-1}.
a_{ph} absorption coefficient for phytoplankton, m^{-1}.
b_p scattering coefficient for particulate material, m^{-1}.
E_d downwelling irradiance, W cm^{-2} nm^{-1}.
K_d diffuse attenuation coefficient for downwelling irradiance, m^{-1}.
K_u diffuse attenuation coefficient for upwelling radiance, m^{-1}.
L_u upwelling radiance, W cm^{-2} nm^{-1} sr^{-1}.
R_{rs} remote sensing reflectance, sr^{-1}.
z depth, m.

Acknowledgments. We are grateful to A. Barnard, A. Canaday, M. DuRand, J. Simeon, S. Etheridge, M. K. Talbot, R. Olson, and R. Zaneveld for critical assistance with data collection and processing. This work was supported by the Office of Naval Research Environmental Optics program (grants to HMS and RJO, CSR, and WSP and JRVZ) and the National Aeronautical and Space Administration (grants to HMS). Woods Hole Oceanographic Institution contribution 10383.

References

Agrawal, Y. C., and P. Traykovski, Particles in the bottom boundary layer: Concentration and size dynamics through events, *J. Geophys. Res.*, this issue.

Balch, W. M., R. W. Eppley, M. R. Abbott, and F. M. H. Reid, Bias in satellite-derived pigment measurements due to coccolithophores and dinoflagellates, *J. Plankton Res.*, *11*, 575-581, 1989.

Berwald, J., D. Stramski, C. D. Mobley, and D. A. Kiefer, Effect of Raman scattering on the average cosine and diffuse attenuation coefficient of irradiance in the ocean, *Limnol. Oceanogr., 43*, 564-576, 1998.

Boss, E., W. S. Pegau, J. R. V. Zaneveld, and A. H. B. Barnard, Spatial and temporal variability of absorption by dissolved material at a continental shelf, *J. Geophys. Res.*, this issue.

Bricaud, A., A. Morel, and L. Prieur, Absorption by dissolved organic matter of the sea (yellow substance) in the UV and visible domains, *Limnol. Oceanogr.*, *26*, 43-53, 1981.

Bricaud, A., A. Morel, and L. Prieur, Optical efficiency factors of some phytoplankters, *Limnol. Oceanogr., 28*, 816-832, 1983.

Bricaud, A., A. L. Bedhomme, and A. Morel, Optical properties of diverse phytoplanktonic species: Experimental results and theoretical considerations, *J. Plankton Res., 10*, 851-873, 1988.

Bricaud, A., M. Babin, A. Morel, and H. Claustre, Variability in the chlorophyll-specific absorption coefficients of natural phytoplankton: Analysis and parameterization, *J. Geophys. Res., 100*, 13,321-13,332, 1995.

Carder, K. L., R. G. Steward, G. R. Harvey, and P. B. Ortner, Marine humic and fulvic acids: Their effects on remote sensing of ocean chlorophyll, *Limnol. Oceanogr., 34*, 68-81, 1989.

Chang, G. C. and T. D. Dickey, Optical and physical variability on timescales from minutes to the seasonal cycle on the New England shelf: July 1996 to June 1997, *J. Geophys. Res.*,this issue.

Chang, G. C., T. D. Dickey, and A. J. Williams III, Sediment resuspension over a continental shelf during Hurricanes Edouard and Hortense, *J. Geophys. Res.*, this issue.

Chisholm, S. W., Phytoplankton size, in *Primary Productivity and Biogeochemical Cycles in the Sea*, edited by P. G. Falkowski and A. D. Woodhead, pp. 213-237, Plenum, New York, 1992.

Cleveland, J. S., Regional models for phytoplankton absorption as a function of chlorophyll *a* concentration, *J. Geophys. Res., 100*, 13,333-13,344, 1995.

DeGrandpre, M. D., A. Vodacek, R. K. Nelson, E. J. Bruce, and N. V. Blough, Seasonal seawater optical properties of the U.S. Middle Atlantic Bight, *J. Geophys. Res., 101*, 22,727-22,736, 1996.

Dickey, T. D., and A. J. Williams III, Interdisciplinary ocean process studies on the New England shelf, *J. Geophys. Res.*, this issue.

Dickey, T. D., G. C. Chang, Y. C. Agrawal, A. J. Williams III, and P. S. Hill, Sediment resuspension in the wakes of Hurricanes Edouard and Hortense, *Geophys. Res Lett.*, *25*, 3133-3536, 1998.

Doerffer, R., and J. Fischer, Concentrations of chlorophyll, suspended matter, and gelbstoff in case II waters derived from satellite Coastal Zone Color Scanner data with inverse modeling methods, *J. Geophys. Res.*, *99*, 7457-7466, 1994.

Dubinsky, Z., P. G. Falkowski, and K. Wyman, Light harvesting and utilization by phytoplankton, *Plant Cell Physiol.*, *27*, 1335-1349, 1986.

Gardner, W.D., et al., Optics, particles, stratification, and storms on the New England continental shelf, *J. Geophys. Res.*, this issue.

Gordon, H. R., O. B. Brown, R. H. Evans, J. W. Brown, R. C. Smith, K. S. Baker and D. K. Clark, A semianalytic radiance model of ocean color, *J. Geophys. Res*, *93*, 10,909-10,924, 1988.

Hill, P. S., G. Voulgaris, and J. H. Trowbridge, Controls on floc size in a continental shelf bottom boundary layer, *J. Geophys. Res.*, this issue.

Hochman, H. T., F. E. Müeller-Karger, and J. J. Walsh, Interpretation of the Coastal Zone Color Scanner signature of the Orinoco River plume, *J. Geophys. Res.*, *99*, 7443-7455, 1994.

Holligan, P. M., M. Viollier, D. S. Harbour, P. Camus, and M. Champagne-Philippe, Satellite and ship studies of coccolithophore production along a continental shelf edge, *Nature*, *304*, 339-342, 1983.

Iturriaga, R., and D. A. Siegel, Microphotometric characterization of phytoplankton and detrital absorption in the Sargasso Sea, *Limnol. Oceanogr.*, *34*, 1706-1776, 1989.

Iturriaga, R., A. Morel, C. Roesler, and D. Stramski, Individual and bulk analysis of the optical properties of marine particulates: Examples of merging these two scales of analysis, in *Particle Analysis in Oceanography*, edited by S. Demers, pp. 339-347, Springer-Verlag, New York, 1991.

Kirk, J. T. O., *Light and Photosynthesis in Aquatic Ecosystems,* 2nd ed., 509 pp., Cambridge Univ. Press, New York, 1994.

Kishino, M., N. Takahashi, N. Okami, and S. Ichimura, Estimation of the spectral absorption coefficients of phytoplankton in the sea, *Bull. Mar. Sci.*, *37*, 634-642, 1985.

Marra, J., R. W. Houghton, and C. Garside, Phytoplankton growth at the shelf-break front in the Middle Atlantic Bight, *J. Mar. Res.*, *48*, 851-868, 1990.

Mitchell, B. G., and D. A. Kiefer, Chlorophyll *a* specific absorption and fluorescence excitation spectra for light-limited phytoplankton, *Deep Sea Res., Part I*, *35*, 639-663, 1988.

Morel, A., Optical modeling of the upper ocean in relation to its biogenous matter content (Case I waters), *J. Geophys. Res.*, *93*, 10749-10768, 1988.

Morel, A., and L. Prieur, Analysis of variations in ocean color, *Limnol. Oceanogr.*, *22*, 709-722, 1977.

Morrison, J. R., Variability of natural fluorescence and its applicability to phytoplankton biomass and photosynthesis prediction: In situ evidence of quenching mechanisms, Ph.D. thesis, Univ. of Wales, Bangor, Wales, U.K., 1999.

Mueller, J. L., and R. W. Austin, Ocean optics protocols for SeaWiFS validation, revision 1, *NASA Tech. Memo., 104566,* 67 pp., 1995.

Nelson, J. R., and S. Guarda, Particulate and dissolved spectral absorption on the continental shelf of the southeastern United States, *J. Geophys. Res.*, *100*, 8715-8732, 1995.

O'Reilly, J. E., and C. Zetlin, Seasonal, horizontal, and vertical distribution of phytoplankton chlorophyll a in the northeast U.S. continental shelf ecosystem, *NOAA Tech. Rep. 139*, 126 pp., Fishery Bulletin, Nat. Mar. Fish. Serv., Springfield, Va., 1998.

O'Reilly, J. E., C. Evans-Zetlin, and D. A. Busch, Primary production, in *Georges Bank*, edited by R. H. Backus and D. W. Bourne, pp. 220-233, MIT press, Cambridge, Mass., 1987.

Pegau, W. S., D. Gray, and J. R. V. Zaneveld, Absorption and attenuation of visible and near-infrared light in water: Dependence on temperature and salinity, *Appl. Opt.*, *36*, 6035-6046, 1997.

Roesler, C. S., Theoretical and experimental approaches to improve the accuracy of particulate absorption coefficients derived from the quantitative filter technique, *Limnol. Oceanogr.*, *43*, 1649-1660, 1998.

Roesler, C. S., and M. J. Perry, In situ phytoplankton absorption, fluorescence emission, and particulate backscattering spectra determined from reflectance, *J. Geophys. Res.*, *100*, 13,279-13,294, 1995.

Roesler, C. S., M. J. Perry, and K. L. Carder, Modeling in situ phytoplankton absorption from total absorption spectra in productive inland marine waters, *Limnol. Oceanogr.*, *34*, 1510-1523, 1989.

Ryan, J. P., J. A. Yoder, and P. C. Cornillon, Enhanced chlorophyll at the shelfbreak of the Mid-Atlantic Bight and Georges Bank during the spring transition, *Limnol. Oceanogr.*, *44*, 1-11, 1999a.

Ryan, J. P., J. A. Yoder, J. Barth, and P. C. Cornillon, Chlorophyll enhancement and mixing associated with meanders of the shelfbreak front in the Mid-Atlantic Bight, *J. Geophys. Res.*, *104*, 23,479-23,493, 1999b.

Siegel, D. A. and A. F. Michaels, Quantification of non-algal attenuation in the Sargasso Sea: Implications for biogeochemistry and remote sensing, *Deep Sea Res., Part II*, *43*, 321-345, 1996.

Siegel, D. A., A. F. Michaels, J. C. Sorenson, M. C. O'Brien, and M. A. Hammer, Seasonal variability of light availability and utilization in the Sargasso Sea, *J. Geophys. Res.*, *100*, 8695-8713, 1995.

Smith, R. C., and K. S. Baker, Optical classification of natural waters, *Limnol. Oceanogr.*, *23*, 260-267, 1978.

Smith, R. C., and K. S. Baker, The Analysis of ocean optical data, *Proc. SPIE Int. Soc. Opt. Eng.*, *489*, 119-126, 1984.

Smith, R. C., and K. S. Baker, Analysis of ocean optical data II, *Proc. SPIE Int. Soc. Opt. Eng., 637*, 95-107, 1986.

Sosik, H. M. and B. G. Mitchell, Light absorption by phytoplankton, photosynthetic pigments and detritus in the California Current system, *Deep Sea Res., Part I*, *42*, 1717-1748, 1995.

Sosik, H. M., R. E. Green and R. J. Olson, Optical variability in coastal waters of the northwest Atlantic, in *Proc. Ocean Optics XIV*, 1-14, 1998.

Stramski, D., and D. A. Kiefer, Light scattering by microoganisms in the open ocean, *Prog. Oceanogr.*, *28*, 343-383, 1991.

Stramski, D., and C. D. Mobley, Effects of microbial particles on ocean optics: A database of single-particle optical properties, *Limnol. Oceanogr., 42*, 538-549, 1997.

Stramski, D., and A. Morel, Optical properties of photosynthetic picoplankton in different physiological states as affected by growth irradiance, *Deep Sea Res., Part I, 37*, 245-266, 1990.

Strickland, J. D. H., and T. R. Parsons, *A Practical Handbook of Seawater Analysis, Bull. Fish. Res. Board Can. 167*, 2nd ed., 310 pp., Ottawa, Ontario, 1972.

Thompson, D. R., and D. L. Porter, SAR and AVHRR observations during 1996 of Hurricanes Edouard and Hortense, *Rep. JHU/APL SRO-97-12*, 21 pp., Appl. Phys. Lab., Johns Hopkins Univ., Laurel, Md., 1997.

Walsh, J. J., T. E. Whitledge, J. E. O'Reilly, W. C. Phoel, and A. F. Draxler, Nitrogen cycling on Georges Bank and the New York Shelf: a comparison between well-mixed and seasonally stratified waters, in *Georges Bank*, edited by R. H. Backus and D. W. Bourne, pp. 234-246, MIT Press, Cambridge, Mass., 1987.

Yentsch, C. S., and D. A. Phinney, A bridge between ocean optics and microbial ecology, *Limnol. Oceanogr.*, *34*, 1694-1705, 1989.

Zaneveld, J. R. V., J. C. Kitchen, and C. C. Moore, The scattering error correction of reflecting tube absorption meters, Proc. SPIE Soc. Opt. Eng., 2258, 44-55, 1994.

R. E. Green and H. M. Sosik, Biology Department, MS32, Woods Hole Oceanographic Institution, Woods Hole, MA 02543-1049 (rgreen@whoi.edu; hsosik@whoi.edu)

W. S. Pegau, College of Oceanic and Atmospheric Sciences, Oregon State University, Corvallis, OR 97331 (spegau@oce.orst.edu)

C. S. Roesler, Bigelow Laboratory for Ocean Sciences, West Boothbay Harbor, ME 04575 (crc@bigelow.org)

(Received April 29, 1999; revised July 24, 2000;
accepted July 31, 2000.)